Slope Stability 2013 – P.M. Dight (ed)

doi:10.36487/ACG_rep/1308_45_Sainsbury

Three-dimensional analysis of pit slope stability in anisotropic rock masses

D.P. Sainsbury *Mining One Consultants, Australia*

B. Sainsbury *Castlemaine Goldfields Ltd, Australia*

Abstract

Anisotropic and foliated rock masses, the behaviour of which are dominated by closely spaced planes of weakness, present particular difficulties in the assessment of pit slope stability. Various numerical modelling techniques are available that explicitly simulate the joints and discontinuities within an anisotropic rock mass. However, due to the computational intensity of these numerical techniques, it is not practical to explicitly simulate the joint fabric of an entire three-dimensional pit slope for routine stability assessment. In order to simulate the effects of anisotropic rock mass strength and deformation behaviour on pit slope stability, a modelling methodology has been developed to account for rock mass anisotropy and scale effects using a continuum based ubiquitous joint constitutive model. This paper outlines the anisotropic modelling methodology and presents a series of demonstration models that have been used to validate the technique.

1 Introduction

The strength and deformation behaviour of a rock mass is governed strongly by (a) the 'intact' strength of the rock blocks and (b) the presence of planes of weakness such as joints, bedding planes, foliation and other discontinuities. Anisotropic rock mass strength and deformation behaviour results when a significant portion of the discontinuities are aligned in a preferred direction, such as the shale and banded iron formation (BIF) rock masses illustrated in Figure 1.

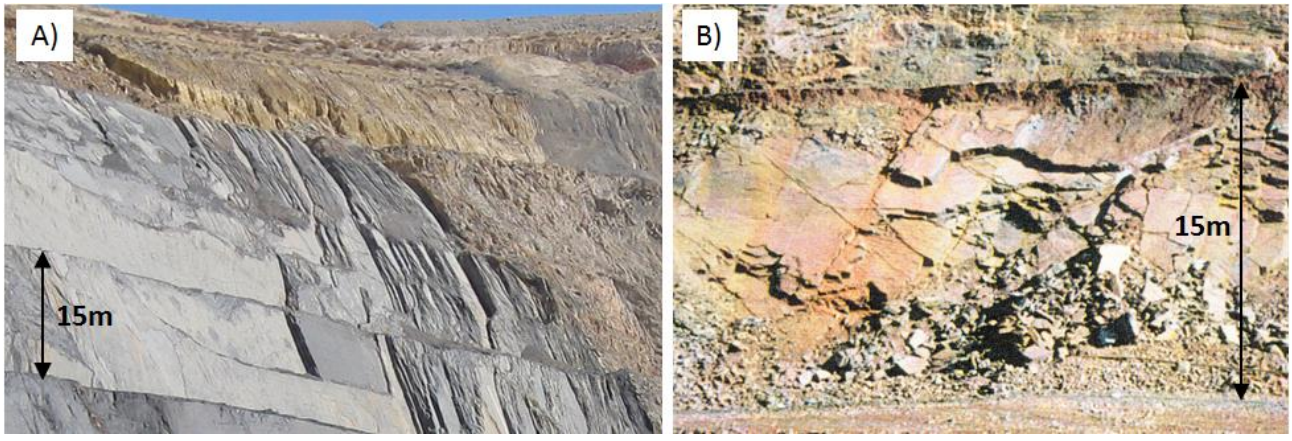

Figure 1 Anisotropic rock masses; (a) shale; and (b) banded iron formation

Various discontinuum modelling techniques are available that explicitly simulate the joint fabric within an anisotropic rock mass. However, due to the computational intensity of these numerical techniques, it is not practical to explicitly simulate the joint fabric of an entire rock mass for routine, large scale, three-dimensional analyses of slope stability. To overcome these issues, the ubiquitous (and subiquitous) Joint constitutive model can be used to represent anisotropic rock masses within continuum-based numerical models (Board et al., 1996; Clark, 2006; Leitner et al., 2006; Sainsbury et al., 2008). The following paper provides a methodology for the simulation of anisotropic rock mass strength and deformation behaviour for use in large scale, three-dimensional pit slope stability analyses.

2 Background

In order to consider the impact of anisotropic rock masses on slope stability, their deformational characteristics must be first quantified. The characterisation of anisotropic strength and deformational behaviour of a number of different rock masses has previously been explored through laboratory triaxial testing on intact specimens by Donath (1972) and McLamore and Gray (1967). Their results are presented in Figure 2. A review of these studies shows that strength varies continuously with the angle of the weakness plane with respect to direction of loading (β). This observation has also been confirmed by many researchers who have studied the behaviour of anisotropic rocks such as shales, slates, sandstone, gneisses and phyllites (Brown et al., 1977; Salcedo, 1983; Singh et al., 1989) along with synthetic cement−based specimens (Tien et al., 2006).

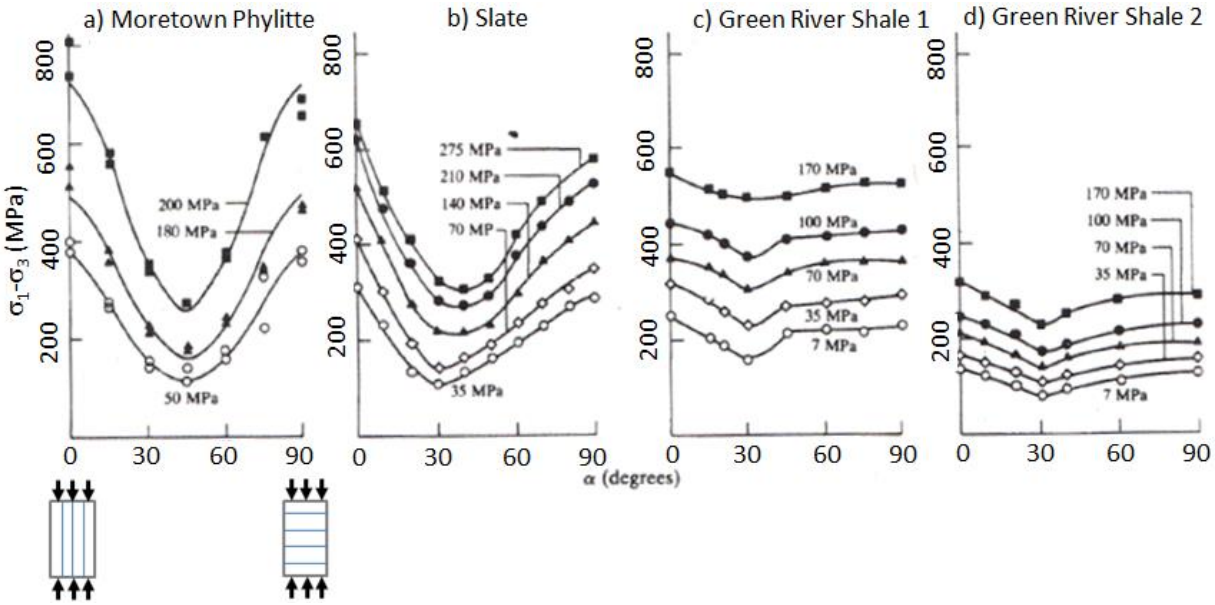

Figure 2 Laboratory testing conducted on anisotropic intact laboratory samples (Donath, 1972; McLamore and Gray, 1967; modified after Brady and Brown, 2004)

Al-Harthi (1998) provides a summary of some idealised anisotropic curves reported throughout the literature. Ideally a single plane of anisotropy, such as joint plane or bedding plane (Figure 3, case I), produces a single U-shape curve with two shoulders. This is consistent with the simple analytical solution developed by Jaeger (1960), which only permits two independent failure modes, i.e. failure along the discontinuity or failure through intact material. A set of discontinuities such as lamination, foliation or cleavage, on the other hand, produces a U- type anisotropy curve with no shoulder (Figure 3, case II).

When considering the numerical analysis of anisotropic rock masses, discontinuum analysis techniques provide the most rigorous assessment of the strength and deformation behaviour. In this case, the actual joint fabric and intact rock bridges are explicitly simulated. However, due to current computational constraints, it is not possible to explicitly simulate the detailed joint fabric that controls anisotropy in large scale three-dimensional pit slopes. As a result of this, ubiquitous (and subiquitous) Joint constitutive models (as implemented in Itasca codes) are commonly used. The ubiquitous Joint model corresponds to a Mohr–Coulomb continuum material that exhibits strength anisotropy due to embedded planes of weakness in each of the zones. The criterion for failure on the plane of weakness consists of a composite Mohr−Coulomb envelope with a tension cut-off.

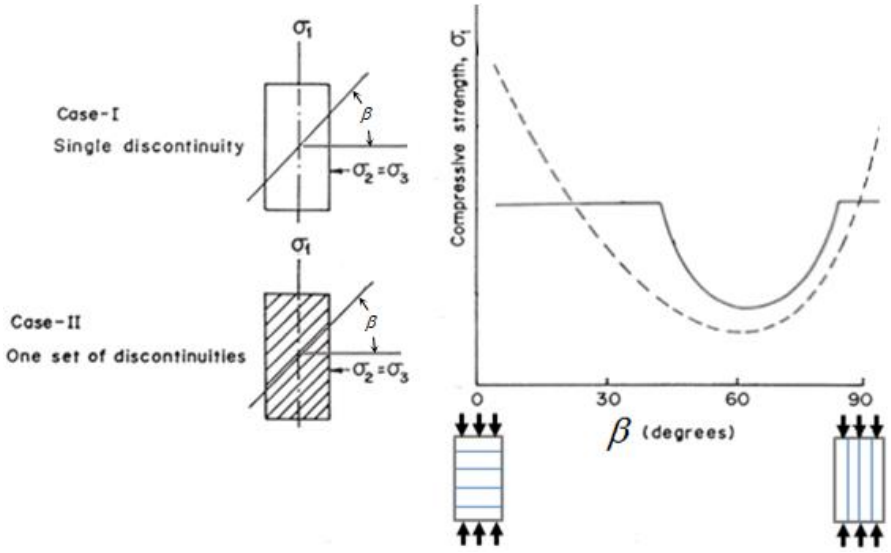

Figure 3 Typical strength anisotropy curves for samples with a single and one set of discontinuities (Al-Harthi, 1998; modified after Hoek and Brown, 1980)

The zone-based matrix and joint properties illustrated in Figure 4 are specified for the model. The subiquitous (strain-softening ubiquitous joint) model is a generalisation of the ubiquitous-joint model which allows a bilinear Mohr–Coulomb failure envelope, together with strain-softening/hardening behaviour for both the matrix and joints. Within both the ubiquitous and subiquitous models, general failure is first detected based upon the Mohr–Coulomb criteria for the matrix. Once the relevant plastic corrections are applied, the new stresses are then analysed for failure on the plane of weakness and updated accordingly.

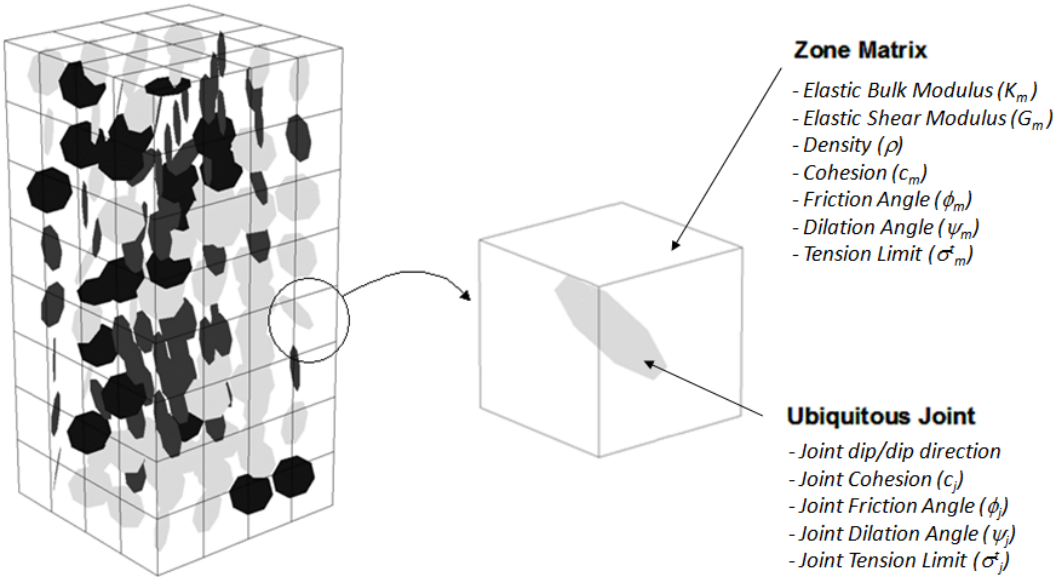

Figure 4 Zone-based matrix and ubiquitous-joint properties

The formulation of ubiquitous joints assumes infinitesimal spacing and no length scale to their implementation. As such, a ubiquitous-joint material cannot account for the bending stiffness of the individual layers of rock. As a result of this, in order to provide meaningful modelling results careful calibration of the matrix and ubiquitous-joint parameters to emergent behaviour from explicit modelling techniques is required. The resultant FLAC3D (Itasca, 2012) modelling methodology has been termed a ubiquitous joint rock mass (UJRM) model. A summary of the calibration process used to develop ubiquitous-joint material properties for large scale slope stability analysis is provided below. A more detailed description of the methodology can be found in Sainsbury and Sainsbury (2013).

3 Development of anisotropic rock mass strength behaviour

Numerical experiments with discontinuum modelling techniques provide significant insight and understanding of rock mechanics processes that are not possible to test in the laboratory due to specimen scale. The following section provides a case-study investigation whereby explicit modelling has been completed and the emergent behaviour has been calibrated in the subiquitous constitutive model for use in large scale pit slope analyses. A generic banded iron formation (BIF) rock mass (as observed in the Pilbara region of Western Australia has been used for the case study (Figure 1(b)).

3.1 Discontinuum modelling

The basic rock mass parameters used to describe the generic BIF material are presented in Table 1. These material properties have been developed based on laboratory testing and in situ characterisation. A detailed description of the constitutive model and the development of the input block and joint properties can be found in Sainsbury and Sainsbury (2013). A brief summary of the typical measureable material properties are provided here for completeness.

Table 1 Basic parameters used to describe BIF material

Rock Mass Properties			Joint Characterisation			
GSI	σ_{ci} (MPa)	m_i	Bedding spacing (m)	c (kPa)	ϕ (deg.)	σ_t (MPa)
60	150	10	0.2	44	33	0.0

A series of large scale (10 m) simulated compression tests have been conducted within the three-dimensional distinct element code 3DEC (Itasca, 2007). A bedding plane spacing of approximately 0.2 m was assigned together with two orthogonal, non-persistent joint sets. The spacing and persistence of the joint sets was assigned to ensure the average block volume within the sample was approximately 0.3 m^3. This is consistent with a GSI of 60 based on Cai et al. (2007). To account for the significant impact that micro-flaws (pores, open cracks, veins) and weathering/alteration can have on strength scale effect, the rock block strength in 3DEC was selected to be 80% of the measured σ_{ci}. This value is based on an empirical scale effect relation for intact rock developed by Hoek and Brown (1980) and extended by Yoshinaka et al. (2008). The characteristic block size as defined by the bedding spacing and GSI value has been used to determine the reduction. Figure 5 illustrates the UCS response of the 3DEC material with a β angle of 0°, which results in a UCS of 81 MPa.

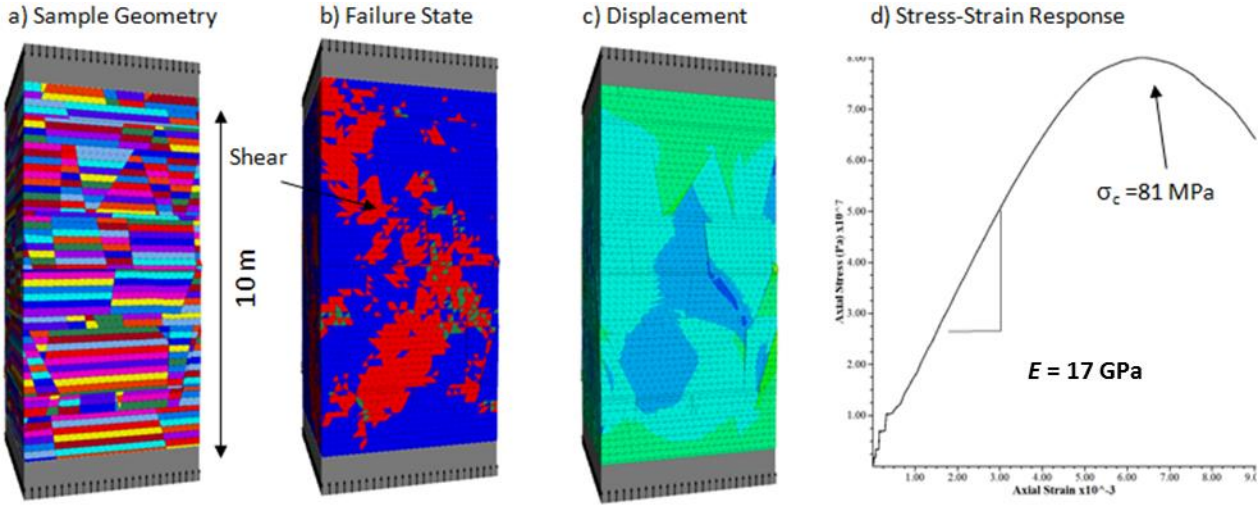

Figure 5 3DEC model of simulated BIF material, β = 0, σ_3 = 0 MPa

A series of UCS and triaxial (σ_3 = 2 MPa) tests were simulated with β angles from 0 to 90°. Figure 6 illustrates the emergent U-shaped strength curve with continuous variability. The strength when β = 90° is predicted to be greater than when β = 0°. This phenomena has also been observed in laboratory triaxial testing on intact specimens reported by Donath (1972) and McLamore and Gray (1967). As illustrated, when β = 90° a tensile splitting mechanism along the bedding develops, while a sliding mechanism along the bedding develops when β = 60°. This behaviour is consistent with the failure mechanisms observed in the laboratory with artificial anisotropic rock described by Tien et al. (2006).

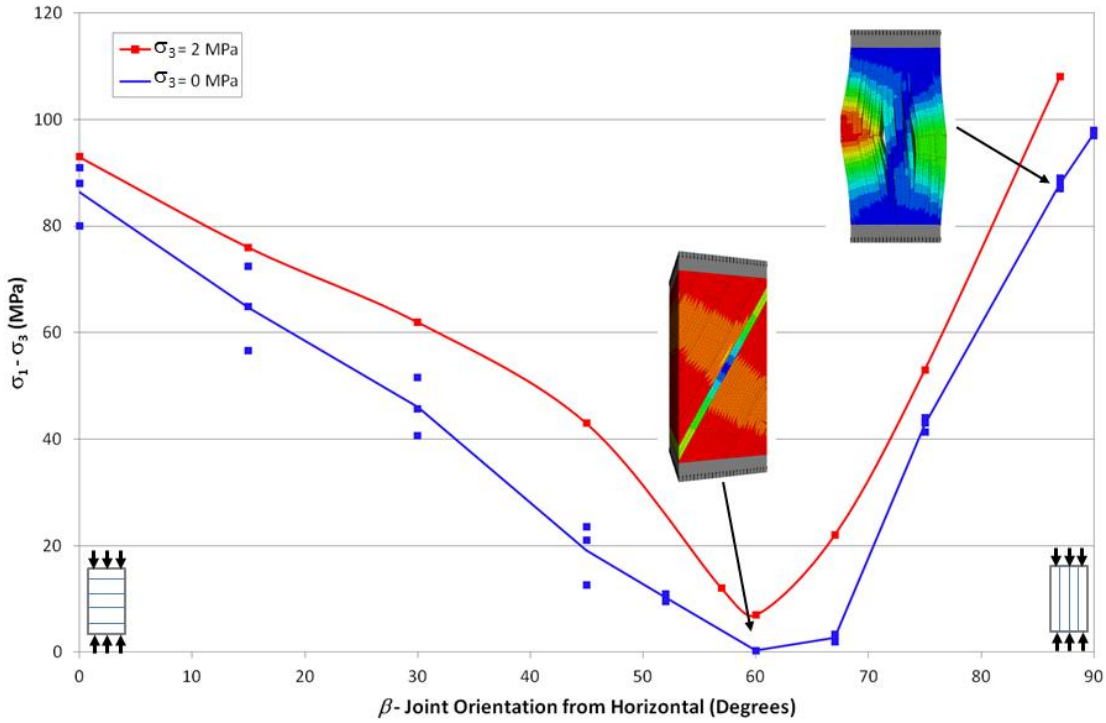

Figure 6 Strength anisotropy curve for simulated BIF material. Upper, lower and average simulation results are shown for the UCS simulations

3.2 Calibration of a ubiquitous joint rock mass (UJRM)

A systematic procedure has been developed to calibrate the subiquitous model to the emergent response of the equivalent discontinuum numerical experiments presented in Figure 6.

The underlying assumptions used in the calibration procedure include:

- The results of the discontinuum analyses more accurately quantify the rock mass anisotropic behaviour than equivalent continuum analyses.
- The actual bedding plane cohesion and friction angle must be used to describe the peak ubiquitous-joint strength to provide a close match to the shear strength of the rock mass under planar sliding conditions.
- The matrix strength and deformation response must be calibrated to help compensate for the lack of length scale and stiffness parameters in the ubiquitous-joint formulation.

3.2.1 Subiquitous model input parameters

3.2.1.1 Orthogonal set of ubiquitous-joints

In order to better represent a naturally occurring anisotropic rock mass, 5 to 20 per cent of the ubiquitous–joints are rotated to be orthogonal to the dominant joint/bedding fabric. The percentage of orthogonal joints represented in the continuum model is determined by the discrete fracture network of

the rock mass and is consistent with the development of the discontinuum model geometry. The inclusion of orthogonal ubiquitous-joints promote continuously variable strength with increasing average β angles. As discussed below, the orthogonal joints help to introduce some bending resistance (i.e. stiffness) within the system when the loading direction is parallel to the ubiquitous joints.

3.2.1.2 Deformation modulus

As discussed, the ubiquitous-joints do not consider the effects of joint stiffness. However, some reduction in the deformation modulus does occur as ubiquitous-joints are mobilised prior to the peak strength. The matrix bulk and shear modulus must be calibrated to best match the deformation modulus of the equivalent discontinuum experiments. The inability of the subiquitous model to account for joint stiffness prevents accurate calibration of the deformation modulus at all β angles.

3.2.1.3 Matrix strength and softening

The peak strength of a subiquitous specimen at β angles of 0 and 90° is dependent on the matrix cohesion, friction and tensile strength. These strength parameters are selected based on a calibration of the matrix material response to the discontinuum strength at a β angle = 0°.

In the interest of simplicity, it is assumed that cohesion and tension soften to zero with accumulated plastic strain. The rate at which softening occurs is calibrated to the post-peak response of the equivalent discontinuum experiment. It is important to note that when introducing softening into the constitutive model, it is important to ensure that the zone size used in the numerical experiment is the same used in the subsequent large scale slope stability simulations.

3.2.1.4 Ubiquitous-joint strength and softening

The actual bedding plane cohesion and friction angle are used to describe the peak ubiquitous-joint strength to provide a close match to the shear strength of the rock mass under planar sliding conditions. Joint cohesion is softened to zero at the same softening rate as the matrix cohesion.

An iterative process is required to calibrate the response of a subiquitous material. Table 2 provides the subiquitous material properties derived to represent the discontinuum material described in Section 3.1.

Table 2 Calibrated subiquitous mechanical properties

Matrix Properties						Ubiquitous-Joint Properties			
E (GPa)	ν	c (MPa)	ϕ (deg.)	σ_t (MPa)	ϵ_{crit}^{ps} (%)	c (kPa)	ϕ (deg.)	σ_t (MPa)	ϵ_{crit}^{ps} (%)
20.4	0.2	14.7	53	1.47	0.016	44	33	0	0.016

The anisotropic strength response of the calibrated subiquitous model is illustrated in Figure 7. The model provides a close match to the continuously variable strength with increasing β angles response provided by the discontinuum analysis.

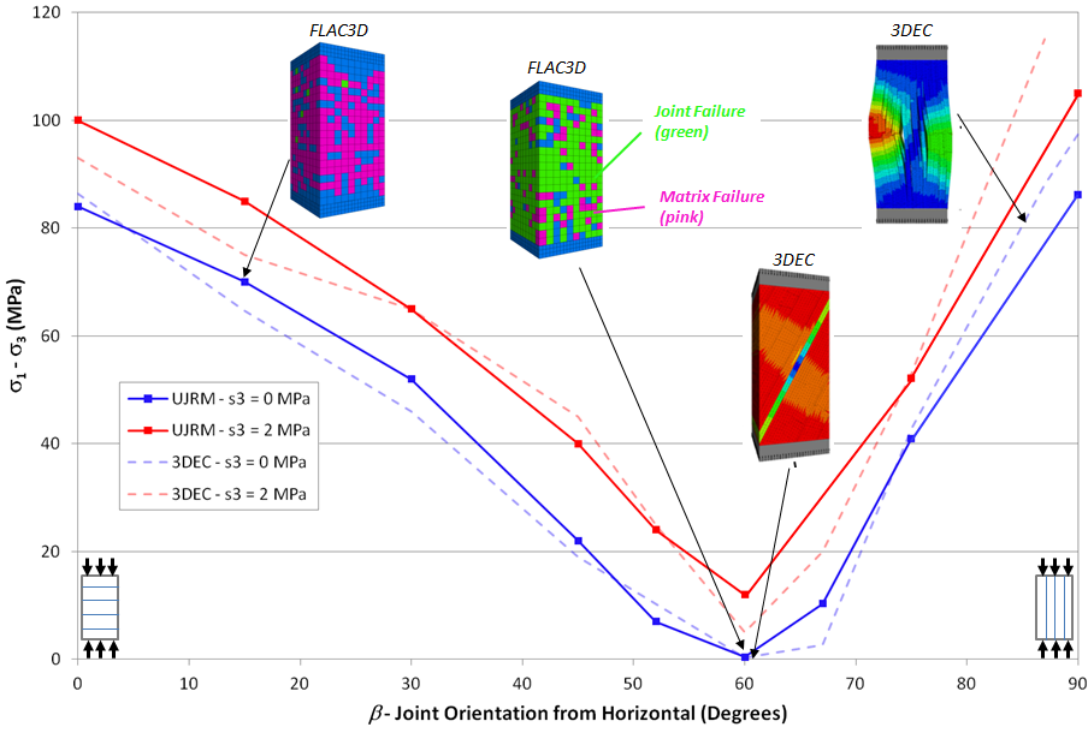

Figure 7 Comparison of 3DEC and FLAC3D-UJRM anisotropic rock mass strength response

The simulated rock mass deformation modulus from the 3DEC and UJRM analyses are presented in Figure 8. The deformation modulus follows a similar continuously variable U-shaped curve to the anisotropic strength response. Modulus values simulated in the vertical (β = 90) direction reflect the input intact modulus (30 GPa). When the modulus is considered perpendicular to the bedding (β = 0) the simulated values are lower than the vertical direction, reflecting the impact of the lower stiffness bedding plane joints.

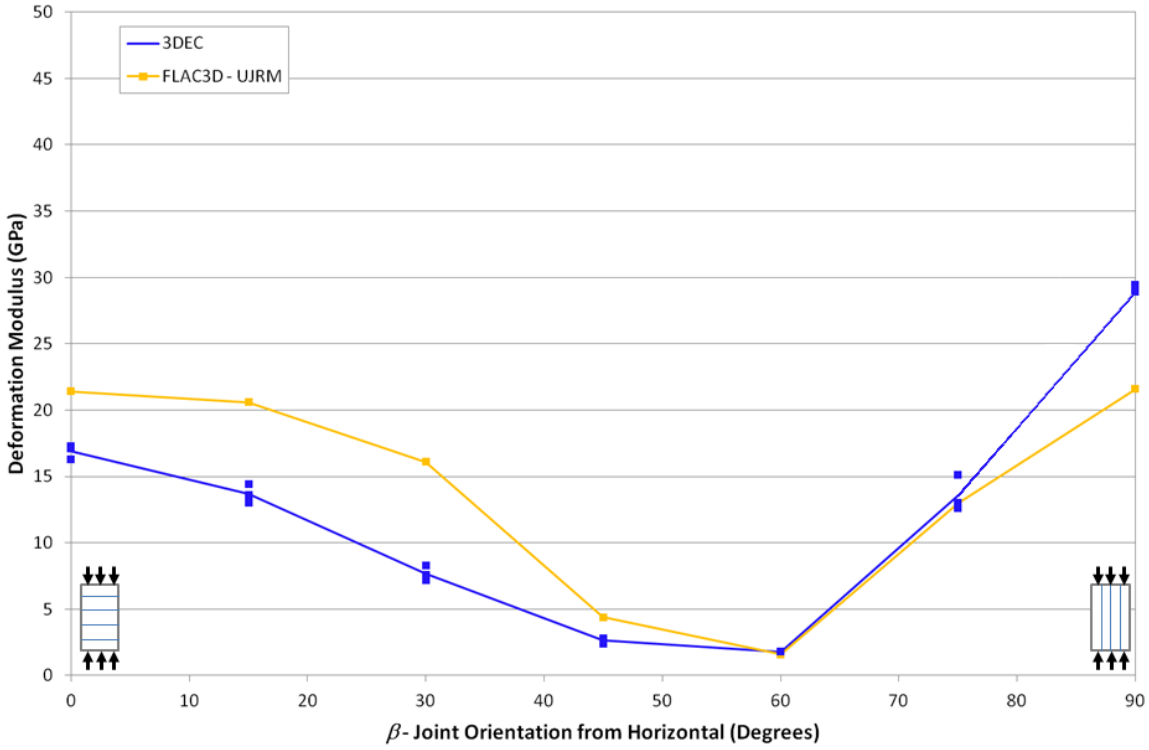

Figure 8 Comparison of 3DEC and UJRM anisotropic deformation modulus response

3.3 Simulation of bedding orientation in three-dimensional slope models

To represent the sometimes extreme folding within sedimentary units exposed in a pit, a routine has been developed to assign the orientation of ubiquitous-joints throughout a large scale pit slope model based on any number of dxf wireframes. Figure 9 illustrates an example model that has been used to study slope stability in anisotropic rock masses. Within these models, large scale explicit structures (representing shale bands) can be simulated directly with interfaces allowing slip and separation according to a Mohr–Coulomb strength criterion. The ubiquitous-joints within each zone have been assigned based upon its proximity to the dxf wireframes of the mapped bedding traces.

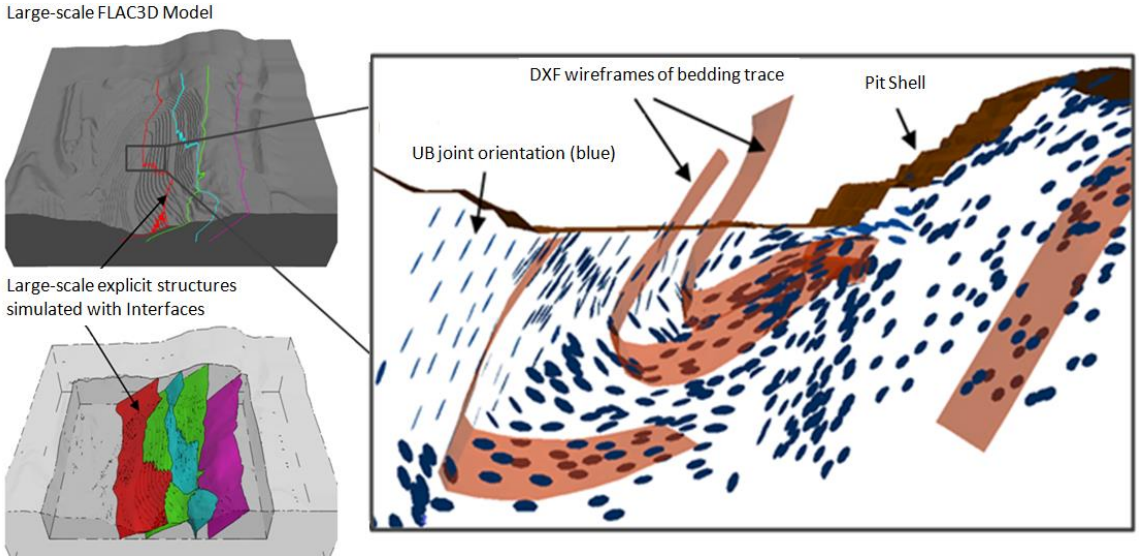

Figure 9 Assignment of ubiquitous-joint orientation (only 1 in 10 joints have been plotted)

4 Demonstration of anisotropic slope failure mechanisms

4.1 Sliding failure mechanisms

The occurrence of slope failure mechanisms controlled by the orientation of weak bedding planes at BHPB's Mt Whaleback Mine was first reported by Kale and Trudinger (1975). Figure 10 illustrates a schematic design section used to assess slope stability within a BIF material. The overall bedding is favourably oriented for stability with exceptions that occur in the synclinal keel areas designated as failure surfaces A, B and C.

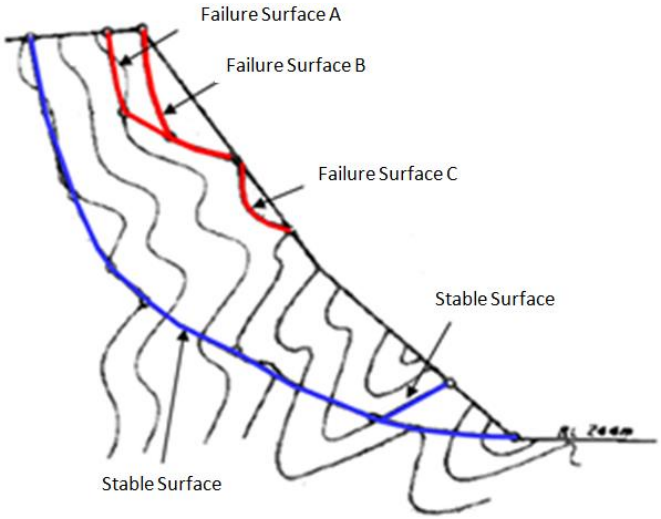

Figure 10 Failure surfaces within design section (after Kale and Trudinger, 1975)

In order to demonstrate the anisotropic behaviour within the slope a pseudo two-dimensional (1 m width) FLAC3D model has been constructed to simulate the basic failure mechanisms reported by Kale and Trudinger (1975). The calibrated UJRM properties developed within Section 3.2 have been used to represent the BIF material. The ubiquitous-joints have been assigned based on a number of conceptual bedding traces that match Figure 10. To provide confidence in the continuum modelling results, a two−dimensional UDEC (Itasca, 2011) model has also been constructed whereby the bedding and cross−joints have been simulated explicitly for comparison. The results of the FLAC3D and UDEC simulations of the slope are presented in Figure 11. The FLAC3D model predicts failure of the synclinal keel areas within the upper portion of the slope providing a close match to the response of the discontinuum model.

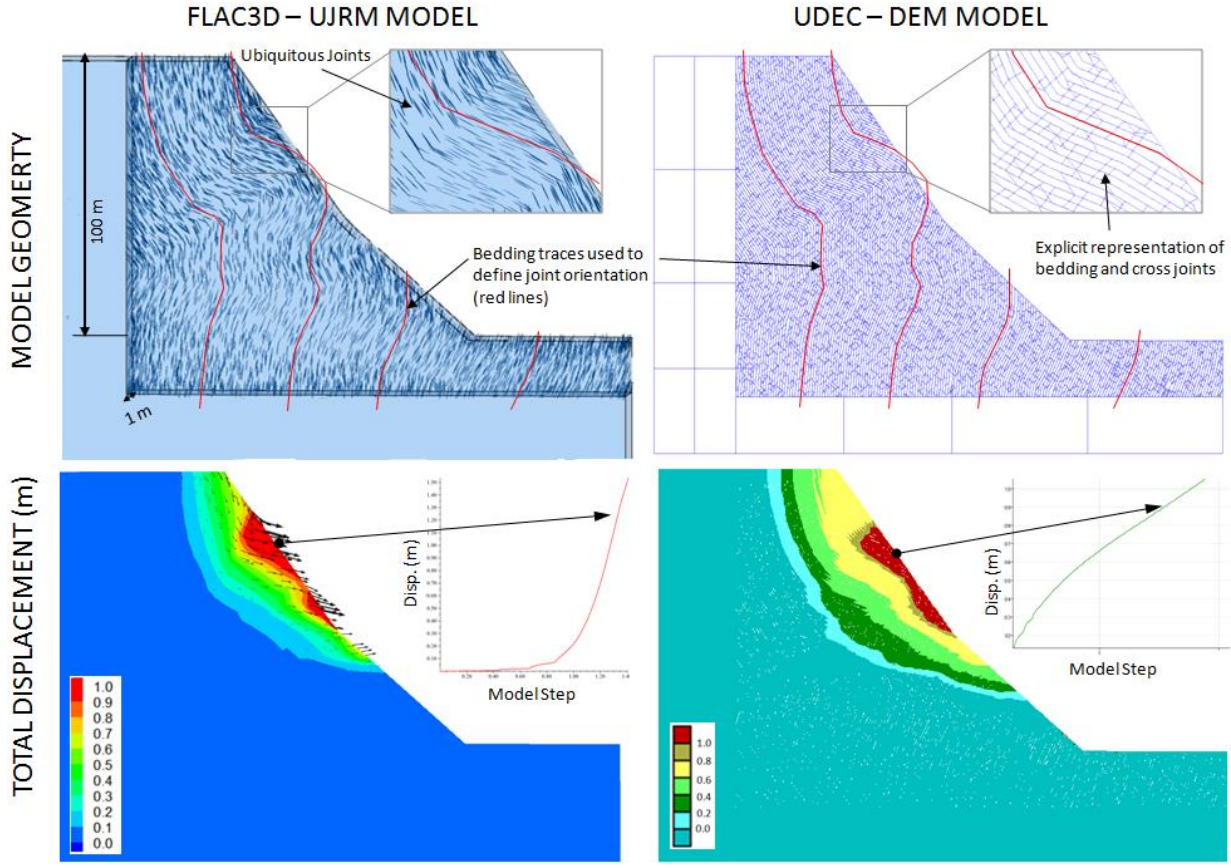

Figure 11 Comparison of FLAC3D-UJRM and UDEC sliding response

4.2 Wedge failure mechanisms

In order to demonstrate the behaviour of a calibrated UJRM model when applied to a simple three-dimensional wedge failure mechanism, a FLAC3D model has been constructed with two opposing ubiquitous joint sets that form a wedge in a 30 m high vertical bench. Figure 12 illustrates the formation of an unstable wedge when the ubiquitous joints are simulated with a cohesion of zero and friction angle less than 30°. The FLAC3D model provides a close match to the analytical solution provided by the SWEDGE program (RocScience, 2013).

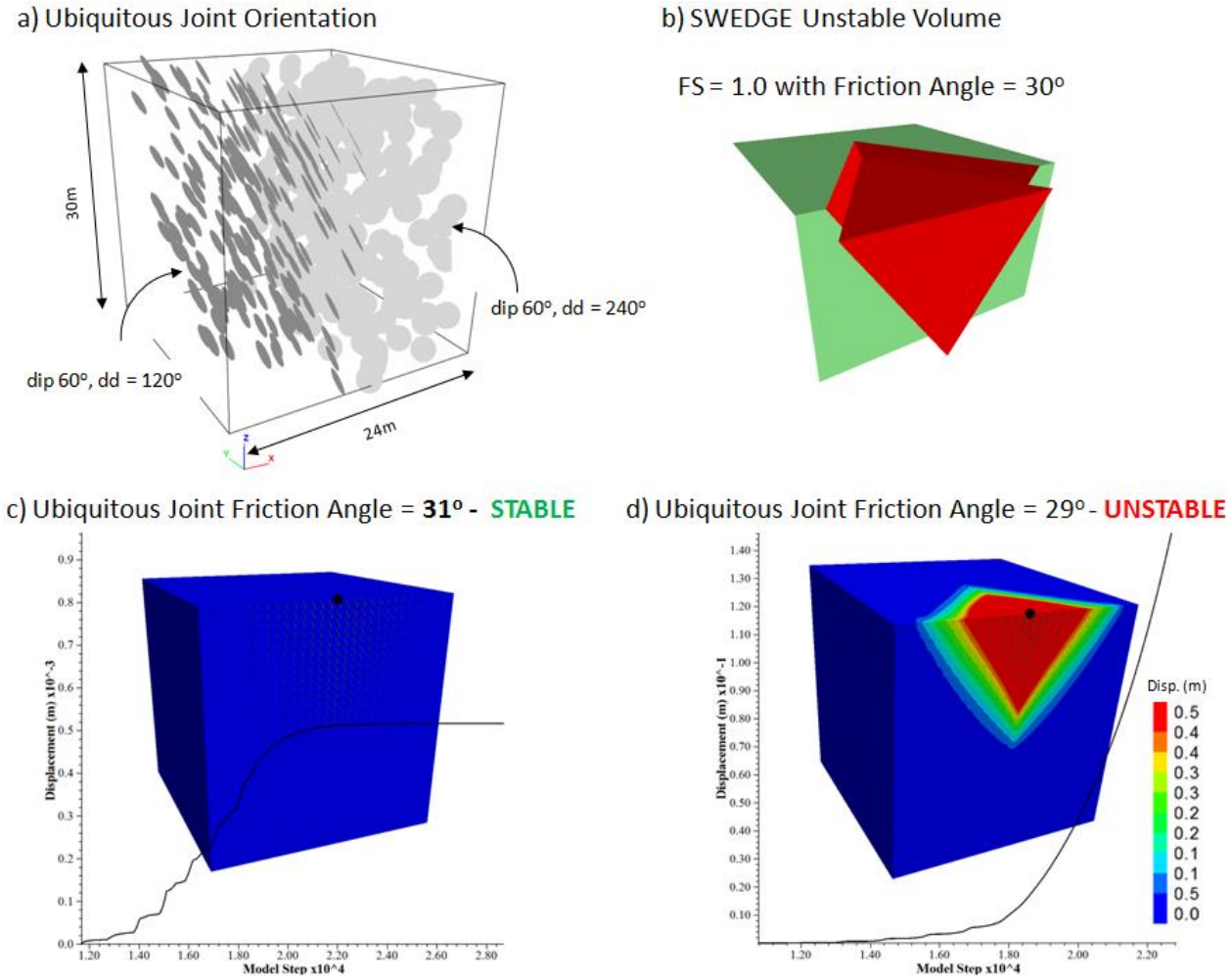

Figure 12 Comparison of FLAC3D-UJRM and UDEC sliding response

4.3 Block toppling mechanisms

The analysis of toppling failure mechanisms presents particular challenges in slope stability analysis. Discontinuum modelling techniques that can explicitly simulate the rotation, translation and bending of individual rock blocks and layers are the most rigorous way to assess slope toppling failure mechanisms. However, the UJRM modelling technique does provide a basic assessment of block toppling failure mechanisms.

In order to demonstrate the toppling response of the calibrated UJRM model discussed in Section 3.2, a FLAC3D model has been constructed with ubiquitous joints dipping 70° into a pit as illustrated in Figure 13. To provide confidence in the modelling results, a two-dimensional UDEC model was also constructed whereby the bedding and cross-joints have been simulated explicitly for comparison. The FLAC3D model predicts the development of instability within the upper portion of the slope, which provides a close match to the response of the instability in the discontinuum model.

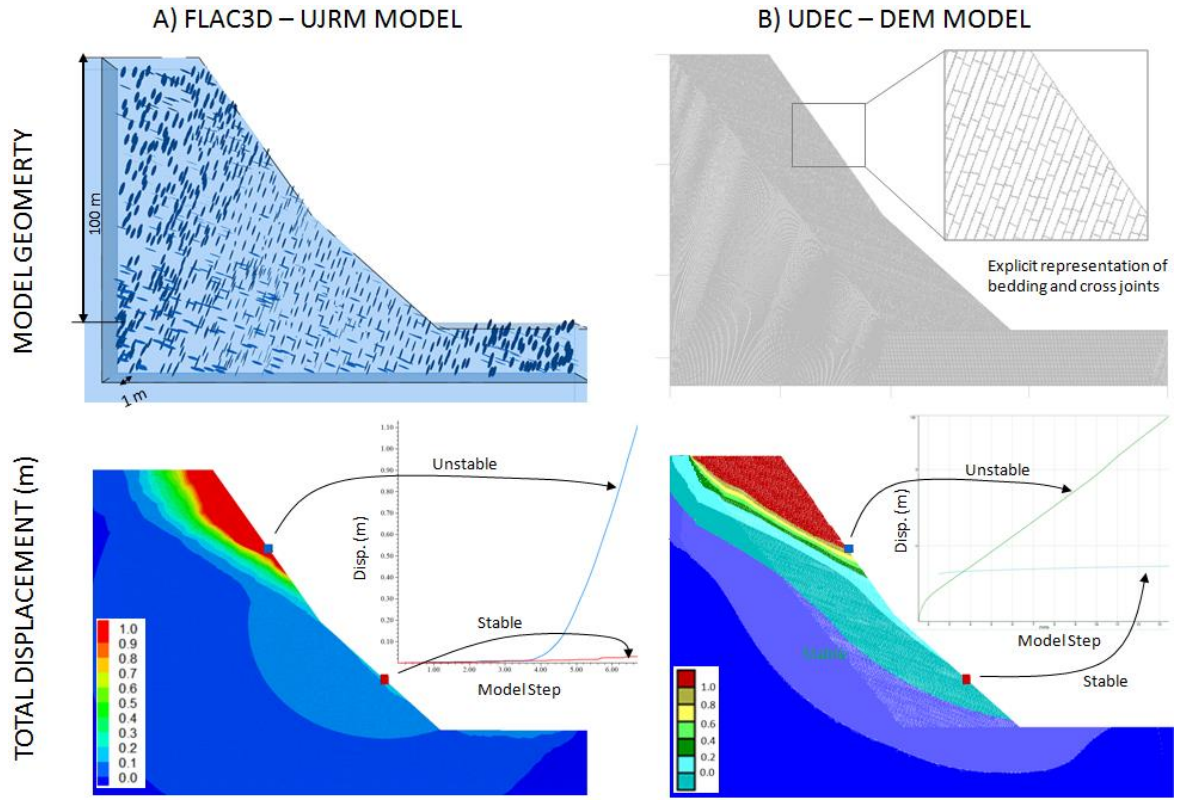

Figure 13 Comparison of FLAC3D-UJRM and UDEC sliding response

Failure mechanisms that involve layer bending, such as flexural toppling, require careful consideration when using a ubiquitous-joint model. As a result of this, it is advisable to conduct parallel discontinuum analyses to ensure meaningful results are achieved.

4.4 Complex non-daylighting wedge mechanisms

Complex non-daylighting wedge failure mechanisms occur in pit slopes whereby anisotropic joint fabric strikes sub-parallel to the pit slope. Figure 14 illustrates a progressive pit slope failure that is controlled by the orientation of shale bedding planes. Observations in situ concluded that low angle bedding (approximately 30° dip) striking sub-parallel to the pit face caused a shallow sliding failure that impacted on the stability of the bench crests. The sliding failure was bounded by a fault that acted as a release surface on one side and a change in bedding orientation on the other. A schematic diagram of the conceptual mode of failure is provided in Figure 14(b).

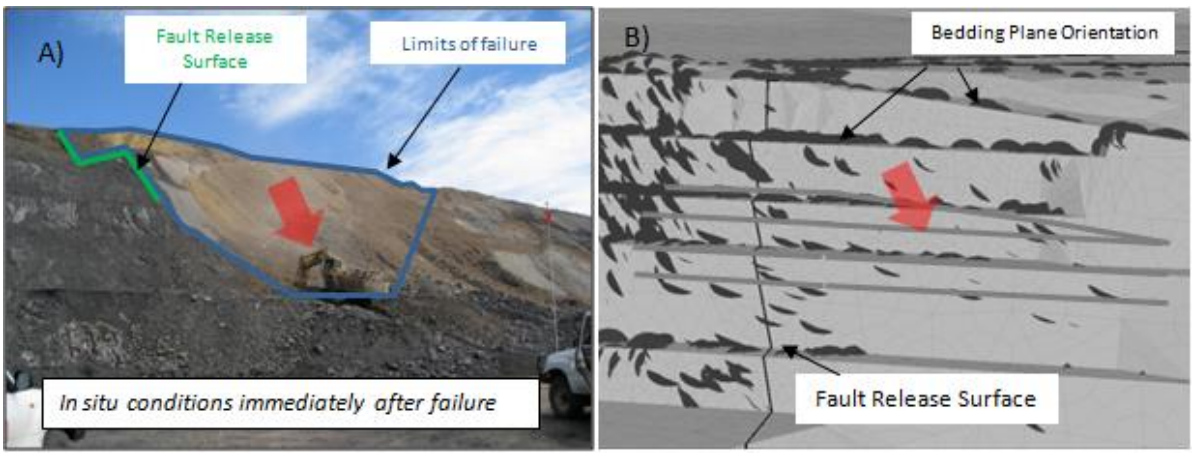

Figure 14 (a) In situ observations immediately after failure; and (b) conceptual model of failure

A three-dimensional numerical analysis of the failure region using an explicit representation of the fault structure and anisotropic rock mass strengths represented by a subiquitous constitutive was developed in FLAC3D. The progressive development of the failure mechanism in the numerical model is provided in Figure 15.

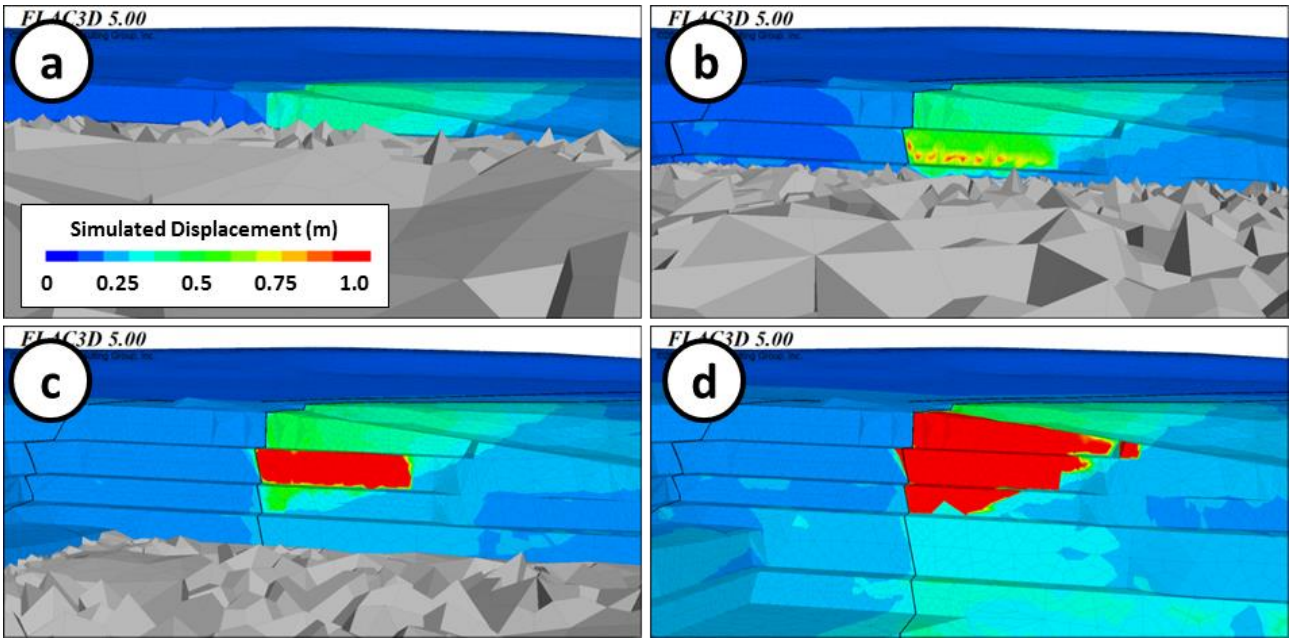

Figure 15 Progressive failure simulated as mining advances in pit

5 Discussion of uncertainties and limitations

Artificial kink bands in ubiquitous-joint models were first reported by Cundall and Fairhurst (1986). The formation of kink-bands and kink-folds are common structures in thinly bedded sedimentary and foliated rocks. Due to the inability of the ubiquitous-joint formulation to represent joint spacing and bending resistance, kink-band formation will always be more pronounced in ubiquitous-joint models.

6 Conclusions

A ubiquitous joint rock mass (UJRM) modelling methodology has been developed to reproduce the directional dependant rock mass strength and deformation behaviour exhibited by anisotropic rock mass domains. The intention of the modelling methodology is to allow a robust stability analysis of anisotropic rock masses using standard mapping and characterisation techniques. The methodology is based on a calibration of a continuum response to the emergent behaviour of discontinuum modelling conducted in a simulated laboratory environment through a number of different stress paths. The modelling methodology has successfully been applied to demonstrate slope failure mechanisms observed in simple anisotropic slope geometries.

Acknowledgement

The assistance of Yoann Hebert in implementing the routine to assign ubiquitous joints based on a dxf file is greatly appreciated.

References

Al-Harthi, A.A. (1998) Effect of planar structures on the anisotropy of Ranyah sandstone, Saudi Arabia. Engineering Geology, Vol. 50, pp. 49–57.

Board, M., Chacon, E., Varona, P. and Lorig, L. (1996) Comparative Analysis of Toppling Behaviour at Chuquicamata Open-Pit Mine, Chile, Transactions Institute of Mining and Metallurgy, Vol. 105(a), January–April 1996, pp. A11–A21.

Brady, B.H.G and Brown, E.T. (2004) Rock Mechanics for Underground Mining, 3rd Edition, Springer, 614 p.

Brown, E.T., Richards, L.R. and Barr, M.V. (1977) Shear strength characteristics of delabole slates, in Proceedings Conference on Rock Engineering, P.B. Attewell (ed), University of Newcastle upon Tyne, UK, pp. 33–51.

Cai, M., Kaiser, P.K., Tasaka, Y. and Minami, M. (2007) Determination of residual strength parameters of jointed rock masses using the GSI system, International Journal of Rock Mechanics and Mining Sciences, Vol. 44, pp. 247–265.

Clark, I. (2006) Simulation of rock mass strength using ubiquitous-joints, Numerical Modeling in Geomechanics – 2006, in Proceedings 4th International FLAC Symposium, R. Hart and P. Verona (eds), 29–31 May 2006, Madrid, Spain, Itasca, Minneapolis, pp. 07–08.

Cundall, P.A. and Fairhurst, C. (1986) Correlation of discontinuum models with physical observations – an approach to the estimation of rock mass behaviour, Felsbau 4, No. 4, pp. 197–202.

Donath, F.A. (1972) Effects of cohesion and granularity on deformational behaviour of anisotropic rock, Studies in Mineralogy and Precambrain Geology, Geological Society of America Memoirs, Vol. 135, pp. 95–128.

Hoek, E. and Brown, E.T. (1980) Underground Excavations in Rock, London, Institution of Mining and Metallurgy, 527 p.

Itasca (2012) FLAC3D, Fast Lagrangian Analysis of Continua in Three-Dimensions, Itasca, Minneapolis, Version 5.0, http://www.itascacg.com/software/flac3d.

Itasca (2011) UDEC, Universal Distinct Element Code, Version 5.0, Itasca, Minneapolis, http://www.itascacg.com/udec.

Itasca (2007) 3-Dimensional Distinct Element Code, Version 4.0, http://www.itascacg.com/software/3dec.

Jaeger, J.C. (1960) Shear failure of anisotropic rocks, Geological Magazine, Vol. 97, pp. 65–72.

Kale, S.M. and Trudinger, J.P. (1975) Slope stability investigations at the Mt Whaleback iron ore mine, Western Australia, in Proceedings SA Conference 1975, June 1975, The Australasian Institute of Mining and Metallurgy, Part B: Whyalla, Leigh Creek, and Adelaide, pp. 571–583.

Leitner, R., Potsch, M. and Schubert, W. (2006) Aspects on the Numerical Modeling of Rock Mass Anisotropy in Tunneling, Felsbau 24, No. 2, pp. 59–65.

McLamore, R. and Gray, K.E. (1967) The mechanical behaviour of anisotropic sedimentary rocks, Journal of Energy for Industry, Transactions of the American Society of Mechanical Engineers, Ser. B, Vol. 89, pp. 62–73.

RocScience (2013) SWEDGE Version 5.0, Toronto, Canada, http://www.rocscience.com/products/9/Swedge.

Sainsbury, B., Pierce, M. and Mas Ivars, D. (2008) Analysis of Caving Behaviour Using a Synthetic Rock Mass – Ubiquitous-joint Rock Mass Modelling Technique, in Proceedings First Southern Hemisphere International Rock Mechanics Symposium (SHIRMS), Y. Potvin, J. Carter, A. Dyskin and R. Jeffrey (eds), Vol. 1 – Mining and Civil, 16–19 September 2008, Perth, Australia, Australian Centre for Geomechanics, Perth, pp. 243–523.

Sainsbury, D. and Sainsbury, B. (2013) Practical use of the Ubiquitous-Joint constitutive model for the simulation of anisotropic rock masses, in Proceedings 3rd International FLAC/DEM Symposium, M. Nelson (ed), 22–24 October 2013, Hangzhou, China, Itasca, Minneapolis (submitted).

Salcedo, D.A. (1983) Macizos Rocosos: Caracterización, Resistencia al Corte y Mecanismos de Rotura, in Proceedings 25 Aniversario Conferencia Soc. Venezolana de Mecánica del Suelo e Ingeniería de Fundaciones, Caracas, pp. 143–172.

Singh, J., Ramamurth, T. and Venkatappa, R.G. (1989) Strength anisotropies in rocks, Indian Geotechnical Journal, Vol. 19(2), pp. 147–166.

Tien, Y.M., Kuo, M.C and Juang, C.H. (2006) An experimental investigation of the failure mechanism of simulated transversely isotropic rocks, International Journal of Rock Mechanics and Mining Sciences, Vol. 43, pp. 1163–1181.

Yoshinaka, R., Osada, M., Park, H., Sasaki, T. and Sasaki, K. (2008) Practical determination of mechanical design parameters of intact rock considering scale effect, Engineering Geology, Vol. 96, pp. 173–186.